Current Science
CS 5 (5), 5049-5061 (2025)
Received 15 July 2025 | **Revised 22 August** 2025 | **Accepted 20 September** 2025 | **Online Available 25 October** 2025
https://doi.org0/10.52845/CS/2025-5-5-53

Current Science
Current Science

OPEN ACCESS
ISSN(O)2795-8639

Original Article

A Novel Signature of Immune- and Inflammation-Related Genes to Predict Prognosis of Hepatocellular Carcinoma

Xuzhou Feng[1], Yunji Xu[1], Wenbing Li[1]

[1]Department of General Surgery, The Second Affiliated Hospital, Hengyang Medical College, University of South China, Hengyang, Hunan,421001, China

***Corresponding Author: Wenbing Li**

Abstract:

Background: Hepatocellular carcinoma (HCC) progression correlates with immune dysfunction and systemic inflammation, necessitating novel immune-inflammatory biomarkers for prognosis.

Methods: This study integrated transcriptomic and clinical data from TCGA-LIHC and ICGC-LIRI-JP cohorts. Immune-inflammatory differentially expressed transcripts (DETs, |log2FC|>2, FDR<0.05) were identified using limma, followed by univariate Cox analysis. An 8-gene prognostic model was constructed via LASSO-Cox regression. Model validation included Kaplan-Meier analysis, time-dependent ROC (timeROC), PCA/t-SNE (Rtsne), and external ICGC validation. Functional enrichment (GSEA/ssGSEA) assessed pathways. Drug sensitivity correlations were analyzed using NCI-60 data. A nomogram integrating genes and clinical features was established (rms package) and calibrated via bootstrap resampling (1000 iterations).

Results: Eleven immune-inflammatory prognostic DEGs (e.g., SLC7A11, MFAP2) were identified. KCNQ3 showed significant OS impact (HR=3.553, P=0.003). The 8-gene model (DNASE1L3, SLC16A3, etc.) stratified high-risk patients with poor OS (TCGA: log-rank P=9.71e-10; ICGC: P=2.278e-04) and high AUCs (1/3/5-year: 0.791/0.727/0.718 in TCGA; 0.730-0.722 in ICGC). Multivariate Cox confirmed risk score as an independent predictor (TCGA: HR=4.210; ICGC: HR=3.189, both P<0.001), correlating with advanced grade (P=2.7e-07) and stage (P=0.00023). Enriched pathways included cell cycle and PI3K-Akt. DNASE1L3-associated genes conferred chemotherapy resistance, while SLC16A3 enhanced ATO sensitivity. The nomogram demonstrated high 1/2/3-year survival prediction accuracy.

Conclusion: Eight immune-inflammatory genes were identified as pivotal prognostic biomarkers for HCC, offering insights into TME dynamics and personalized therapeutic strategies for chemotherapy / immunotherapy.

Keywords: Hepatocellular carcinoma, Immune- and inflammation-related genes, Overall survival, Immune status, Tumor microenvironment, Drug sensitivity

1. Background

Primary liver cancer refers to malignant tumors originating from hepatocytes and intrahepatic bile duct epithelial cells, among which hepatocellular carcinoma (HCC) is the most common type. The global incidence of HCC is 10.1 patients per 100,000 people per year, with East Asia and Africa contributing to 80% [1]. Chronic hepatitis B or C infection, alcohol abuse, fatty liver, and dietary aflatoxins are the high-risk factors for HCC [2]. The management of HCC has markedly improved since early 2010. However, the 5-year survival rate of patients with liver cancer still does not exceed 20%; early diagnosis rate is low, and high recurrence is still an important issue [3-6]. Inflammation and immunity play important roles in the occurrence and development of liver cancer in chronic liver disease [7-8]. Elucidating the immune-inflammatory crosstalk holds

translational value for advancing targeted therapeutic paradigms and circumventing treatment resistance mechanisms in precision oncology [9].

Increasing evidence confirmed that chronic inflammation plays a key role in the pathobiology of cancer, affecting its progression, metastatic potential, and treatment outcomes by altering the tumor immune microenvironment (TME) [10]. During early oncogenesis, canonical Th1-polarized mediators including interferon-gamma (IFN-γ) exert critical immunomodulatory effects that potentiate adaptive antitumor responses. Paradoxically, sustained inflammatory states evolve into chronic pathological processes that fuel neoplastic expansion and metastatic dissemination [11]. The EMT mechanism emerges as a fundamental biological driver of malignant progression, with pleiotropic mediators (TNF-α, IL-1β, IL-6, IL-11, CXCL8) serving as catalytic effectors of this transformative process [12]. Within tumor microenvironments, cytokine networks synergistically orchestrate protumorigenic niches through dual modalities: direct neoplastic cell modulation and dynamic reprogramming of stromal constituents [9].

As dominant immunocytes within the tumor microenvironment, macrophage infiltration density inversely correlates with hepatocellular carcinoma outcomes. These plastic phagocytes undergo polarization into immunostimulatory (M1) or immunosuppressive (M2) phenotypes contingent on microenvironmental cues. M1 variants demonstrate antigen-presenting competence and tumoricidal potential, contrasting with M2 counterparts that secrete immunosuppressive mediators to establish tolerance niches [13]. While innate immunosurveillance mechanisms constrain early neoplastic transformation, subsequent immune-editing processes and stromal dysregulation drive oncogenic evolution [14]. Hepatic NK lymphocytes mediate tumoricidal activity through cytotoxic granule exocytosis and cytokine storm induction, constituting frontline defense effectors [15-17]. Their functional exhaustion establishes permissive conditions for hepatocarcinogenesis, particularly through impaired immunoediting capacity in cirrhotic microenvironments [18].

In this study, we screened differentially expressed genes (DEGs) related to HCC prognosis in the TCGA-LIHC database, and immune- and inflammation-related genes were analyzed. Key genes were identified using Lasso-Cox regression, and prognostic models and nomogram were established from TCGA-LIHC and ICGC-HCC datasets. The prognostic model was used to analyze the correlation between clinical characteristics (age, grade, gender, and stage) and prognosis in liver cancer.

Materials and Methods

2.1 Data Collection and Workflow

The transcriptome data and corresponding clinical data of HCC were collected from TCGA-LIHC (https://portal.gdccancer.gov/repository) and IC GC-LIRI-JP (https://dcc.icgc.org/projects/LIRI-JP) datasets. In total, 546 immune- (humoral) and inflammation-related genes (Systematic name: M8838) were obtained in the molecular signature database from gene set enrichment analysis (GSEA) (http://www.gsea-msigdb.org/gsea/). The workflow was illustrated in Figure 1.

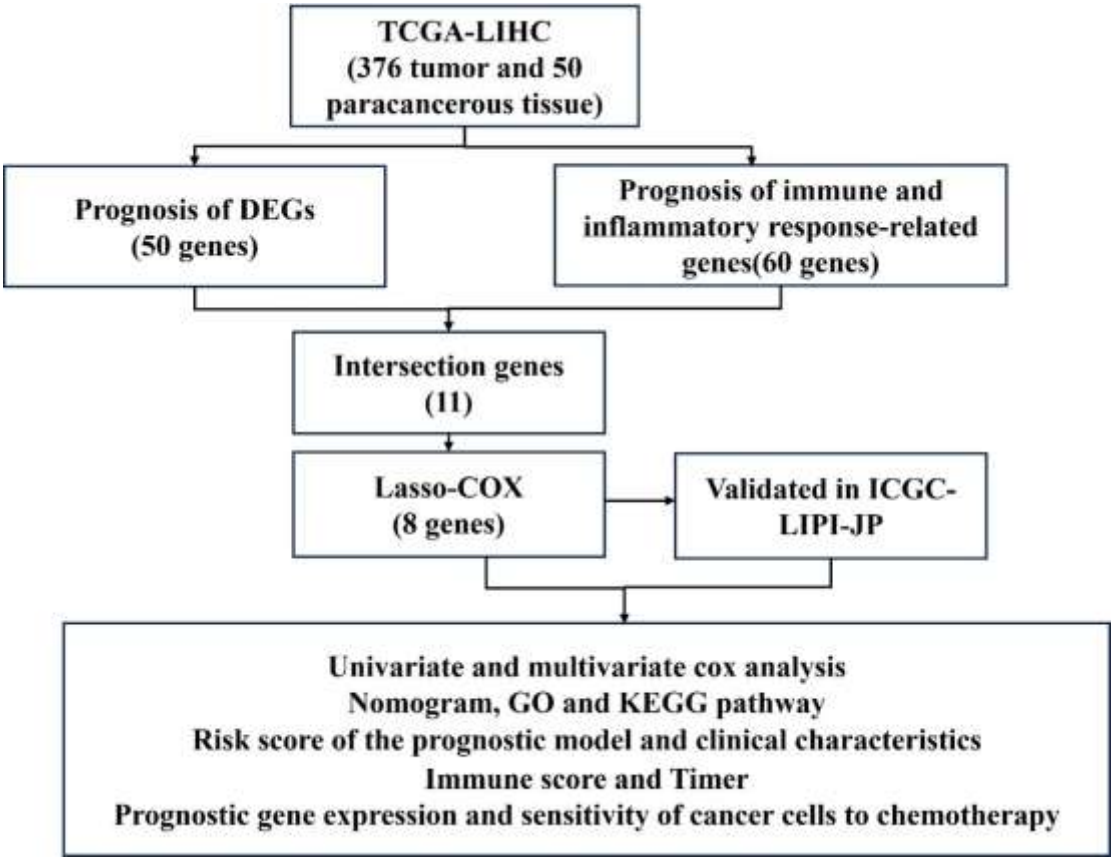

Figure 1, The workflow was illustrated.

2.2 Construction and Verification of the Prognostic Model in HCC

Bioinformatic interrogation of TCGA-LIHC tumor-paracarcinoma transcriptomes was conducted using limma's linear modeling framework, identifying immune-inflammatory differentially expressed transcripts (DETs) under threshold criteria (|log2FC|>2, FDR<0.05). Prognostically significant candidates were selected through univariate survival analysis (OS endpoint). Venn diagrammatic intersection of DETs and survival-associated signatures was performed using the "venn" computational tool. A regularized regression framework (glmnet-implemented LASSO-Cox) integrated temporal survival data with transcriptional profiles to derive prognostic coefficients [19-20]. Individual risk stratification was computed via: Risk Score=∑i=1n(βi·gexi)Risk Score=i=1∑n(βi ·gex$i$). where βiβi represents LASSO-derived coefficients and gexigex$i$ denotes normalized expression values. Cohort stratification into prognostic subgroups (high/low-risk) enabled survival trajectory visualization through Kaplan-Meier methodology (survminer implementation).

ROC curve was plotted using R package "timeROC" to analyze the predictive ability of its characteristic gene prognostic model. Principal component analysis (PCA) and t-distributed random neighbor embedding (t-SNE) analysis were performed, and the two-dimensional visualization of data was performed using the "Rtsne" and "ggplot2" packages. Univariate and multivariate Cox regression analyses were performed, and the "survival" package was used to determine independent prognostic factors. The nominal graph was used to predict the survival probability of patients with HCC with R package "rms."

2.3 Functional Enrichment Analyses

Using Gene Set Enrichment Analysis (GSEA), Gene Ontology (GO) and Kyoto Encyclopedia of Genes and Genomes (KEGG) functional enrichment analyses were performed on the DEGs between the high- and low-risk groups, and functional enrichment analysis was performed on the hallmark genes. Using Single-sample GSEA, 16 immune infiltration scores were calculated and the activity of 13 immune-related pathways was assessed between the high- and low-risk groups with the R package "gsva" [21].

2.4 Analysis of Drug Sensitivity

NCI-60 data of 60 different cancer cell lines from 9 different tumors were collected using CellMiner (https://discover.nci.nih.gov/cellminer). Pearson's correlation analysis was performed to explore the relationship between prognostic gene expression and drug sensitivity.

2.5 Establishment of the nomogram

Eight prognostic biomarkers identified through multivariate regression were integrated into a combinatorial prediction algorithm, forming a clinical nomogram with independent prognostic capacity. Temporal survival patterns were encoded into a machine learning architecture validated by time-dependent ROC analysis (AUC evaluation at 1/2/3-year intervals). Model calibration employed bootstrap resampling (1000 iterations) with Harrell's concordance index (C-index) quantification to ensure predictive fidelity.

2.6 Statistical Analysis

Student's t-test (R function t-test) was performed to determine the significant differences between the two groups. P-value < 0.05 was considered significant. The ggplot package was used for plotting the graphs.

3. Results

3.1 Screening of prognostic immune- and inflammation-related DEGs

In the TCGA-LIHC dataset, 50 DEGs were screened between tumor and nontumor tissues, and 60 immune- and inflammation-related prognostic genes were identified (Figure 2 A). The Venn diagram and heatmap show the expressions for 11 DEGs, including *SLC7A11*, *MFAP2*, *ENTPO2*, *DNASE1L3*, *CCNF*, *STMN1*, *SPP1*, *SLC16A3* (Figure 2 B-C). Univariate Cox analysis revealed that 11 of them were related to OS (Figure 2 D). The hazard ratio (HR) of *KCNQ3* gene was 3.553 (95% CI = 1.552–8.130, P = 0.003, Figure 2 D). The correlation between these genes is shown in Figure 2 E.

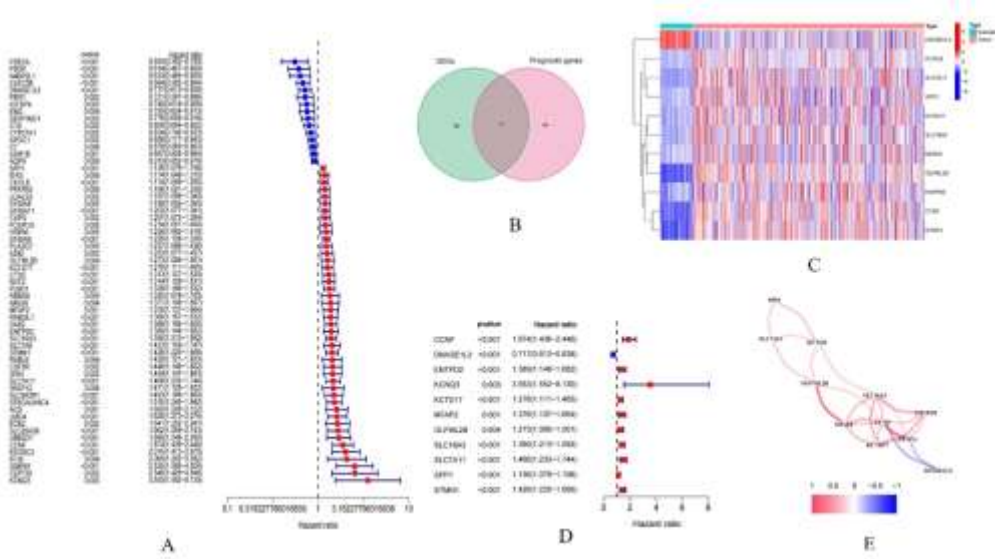

Figure 2, Identification of differentially expressed genes and immune prognostic genes in TCGA-LIHC dataset. (A) Sixty immune- and inflammation-related genes associated with TCGA-LIHC prognosis. (B-C) The Venn diagram and heatmap show the expressions for 11 DEGs. (D) The prognosis and Hazard ratio of 11 intersection genes in TCGA-LIHC dataset. (E) 11 genes correlations and heatmaps in TCGA-LIHC dataset.

3.2 Construction and Verification of the Stability of the Prognostic Model

Through LASSO-regularized Cox regression (λ optimized via cross-validation), eight transcriptional determinants were selected from the discovery cohort (TCGA-LIHC) as multivariate survival predictors (Figure 3 A-D). Risk stratification using median cutoffs revealed pronounced survival dichotomy (log-rank P=9.71e-10), with the low-risk subgroup demonstrating superior clinical outcomes (Figure 3 E). Temporal predictive capacity was evidenced

by sustained AUC metrics (1/3/5-year: 0.791/0.727/0.718) through time-dependent ROC profiling (Figure 3 F). Manifold learning (PCA-tSNE integration) confirmed distinct phenotypic partitioning aligned with risk stratification (Figure 3G-H).

External validation in the ICGC hepatocarcinoma dataset replicated prognostic fidelity (Figure 4 A–B), showing concordant survival divergence (P=2.278e-04, Figure 4 C) and temporal discrimination (AUC 0.730-0.722, Figure 4 D). Manifold learning (PCA-tSNE integration) confirmed distinct phenotypic partitioning aligned with risk stratification (Figure 4 E–F).

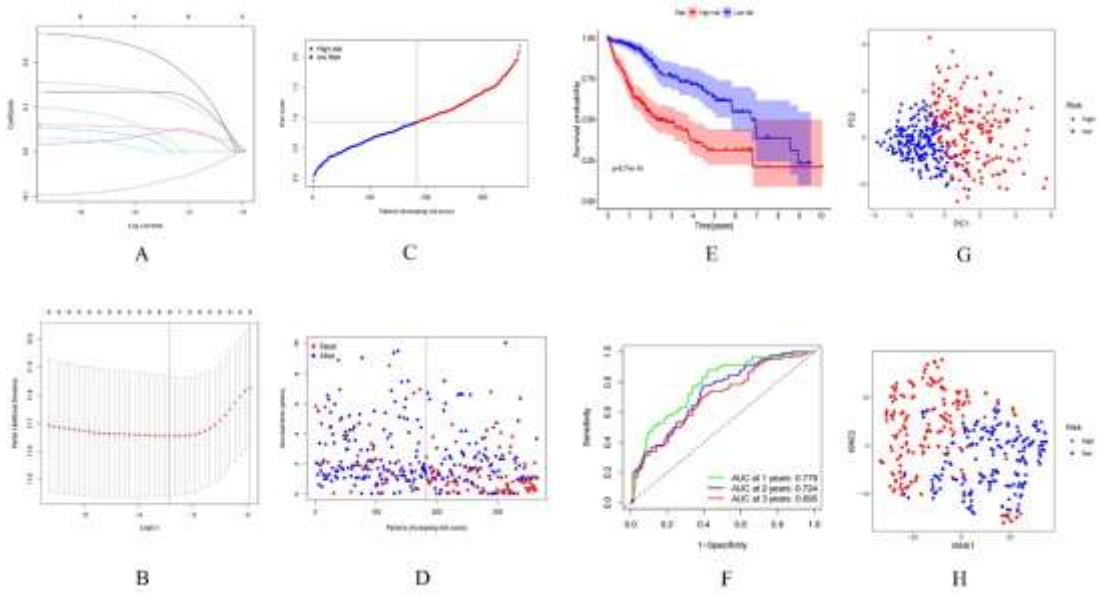

Figure 3, Prognosis value of the 11 intersection genes model in TCGA-LIHC dataset. Distribution of LASSO coefficients of inflammation-related genes in TCGA-LIHC dataset. (B) Partial likelihood deviance against log(λ) is plotted. TCGA and ICGC database: (A) The distribution and median of the risk score. (B) The status of OS and the distribution of risk scores. (C) Kaplan-Meier analysis survival rates for patients in high-risk and low-risk groups. (D) AUC time-dependent ROC curve evaluates the prognosis model for OS. (E) PCA diagram. (F) t-SNE analysis.

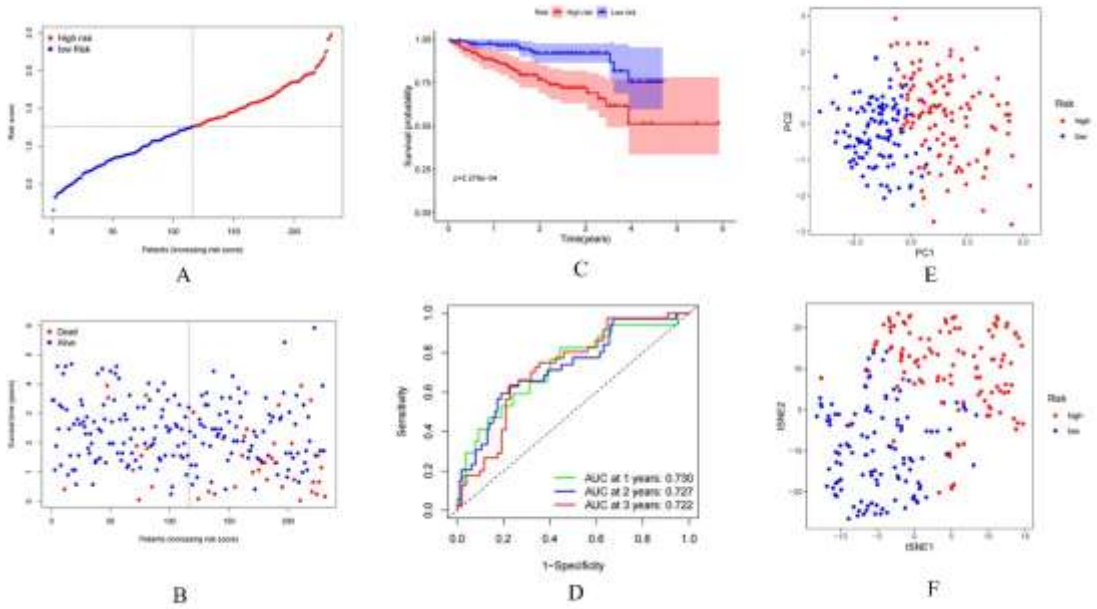

Figure 4, Prognosis value of the 11 intersection genes model in ICGC-(LIRI-JP) dataset. (A) The distribution and median of the risk score. (B) The status of OS and the distribution of risk scores. (C) Kaplan-Meier analysis survival rates for patients in high-risk and low-risk groups. (D)

AUC time-dependent ROC curve evaluates the prognosis model for OS. (E) PCA diagram. (F) t-SNE analysis.

3.3 The Expression and Prognostic Ability of the 8 Genes

The expression of 8 genes is highly expressed in tumors, except for DNASE1L3 (Figure 5 A–H). To explore the relationship between the expression of 8 prognosis-related genes and OS, survival analysis was performed based on the expression value of each gene in HCC form TCGA-LIHC dataset. ENTPD2 was not related with OS. High expression of DNASE1L3 and low expression of remaining 7 genes in tumor tissues were beneficial for the OS of patients (Figure 5 I–P).

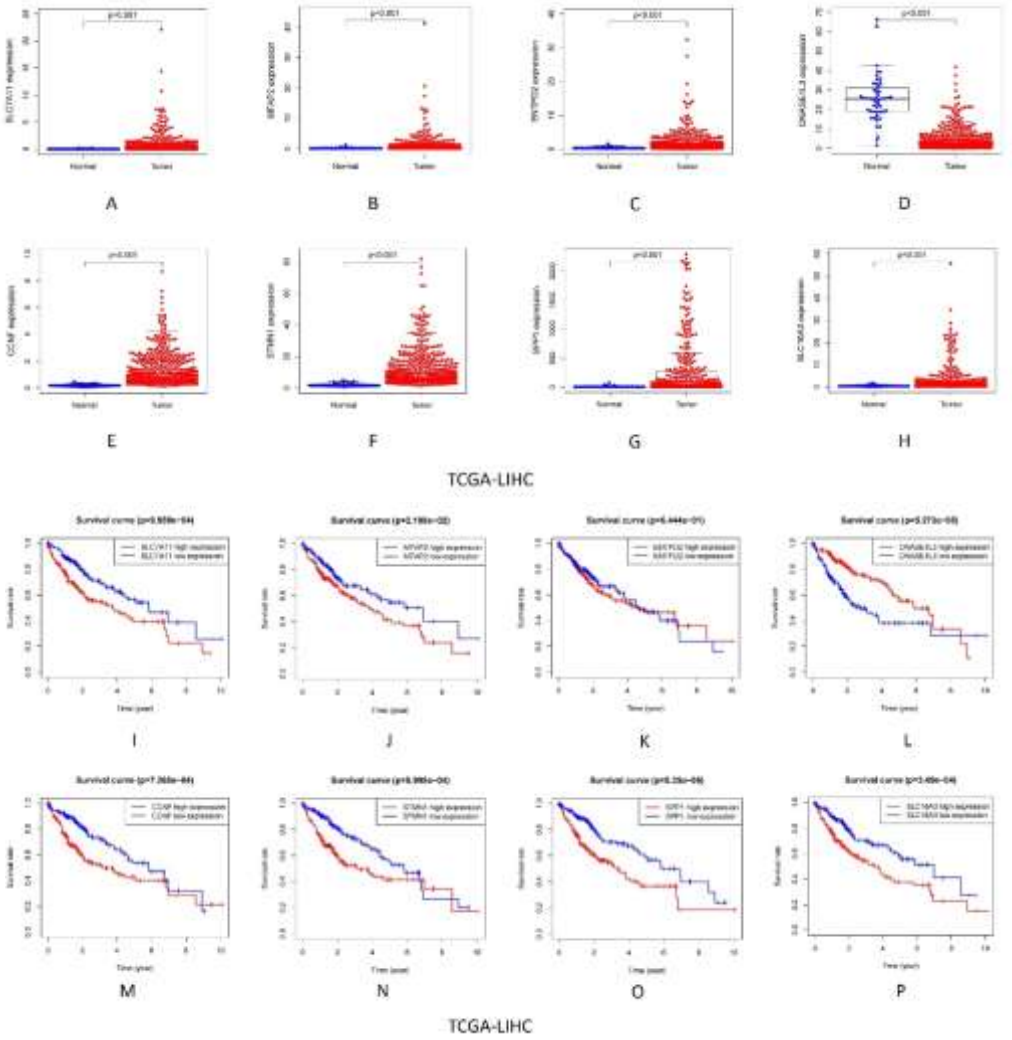

Figure 5, The expression and prognosis of 8 genes in TCGA-LIHC dataset.
(A-H) The expression of 8 genes in tumor and normal tissue. (I-P) The prognosis of 8 genes in patients with high- and low-risk groups.

3.4 Independent Prognostic Analysis of the 8 Genes

Univariate and multivariate Cox analyses were performed on clinical indicators to determine whether the risk score can be used as an independent prognostic predictor of OS. Univariate Cox analysis revealed that the risk-scores in TCGA-LIHC and ICGC-(LIRI-JP) cohorts were significantly correlated with OS (TCGA-LIHC: HR = 4.754, 95% CI = 2.888–7.824, P < 0.001; ICGC- (LIRI-JP): HR = 4.108, 95% CI = 2.221–7.633, P < 0.001) (Figures 6 A, D). Multivariate Cox analysis revealed that risk score was still an independent predictor of OS (TCGA-LIHC: HR = 4.210, 95% CI = 2.430–

7.293, P < 0.001; ICGC-(LIRI-JP): HR = 3.189, 95% CI = 2.211–6070, P < 0.001) (Figures 6 B, E). ROC curve analysis revealed that in the TCGA (AUC = 0.782) and ICGC (AUC = 0.730) datasets (Figures 6 C, F), the risk score had better predictive accuracy for the prognosis of HCC.

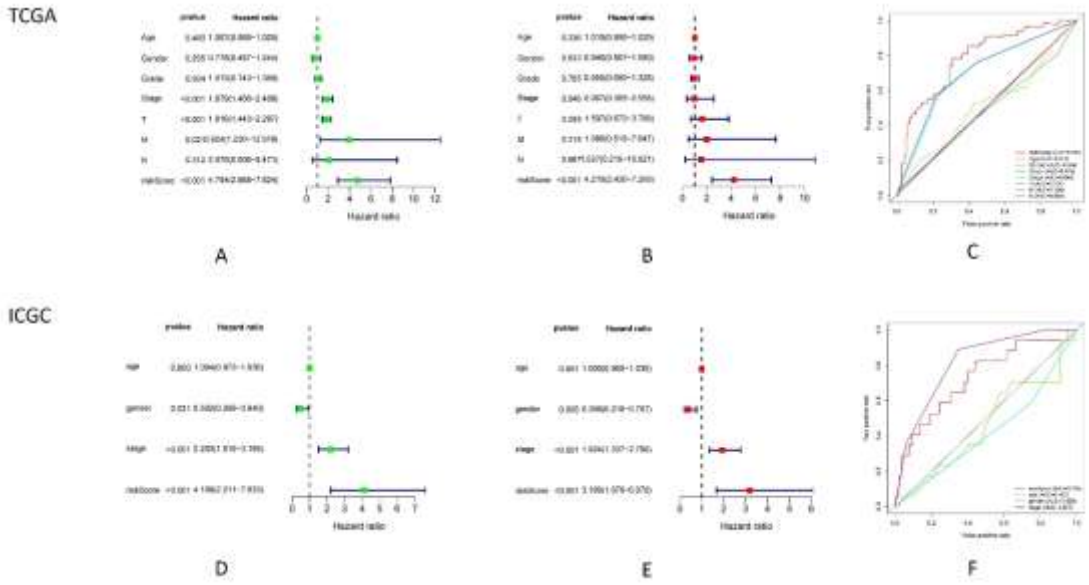

Figure 6, Screening OS-related single factors to compare the prognosis accuracy of risk scores and clinical pathology factors.
TCGA cohort (A-C), ICGC cohort (D-F). (A, D) Screening OS-related factors using Univariate Cox regression analysis. (B, E) Filter OS-related factors using Multivariate Cox regression analysis. (C, F) The prognosis accuracy of risk scoring combined with clinical pathological characteristics was compared using time-dependent ROC curves.

3.5 Relationship between the Risk Score of the Prognostic Model and Clinical Characteristics

The correlation between the risk score and clinical characteristics of patients with HCC was analyzed (Table 1). In TCGA-LIHC dataset, the risk score of age (≤65 vs ＞65) and gender (Female vs male) were no difference(P=0.96 and P=0.93, Figure 7 A, B). However, the risk score was significantly higher for the histological grade 3–4 and TNM stages III–IV than for the histological grade 1–2 and TNM stages I–II, respectively (P =2.7e-07 and P =0.00023, Figures 7 C–D). Interestingly, in ICGC dataset, no significant difference was observed of age and gender (P=0.38 and P=0.7, Figures 7 E–F). Similarly, the risk score of TNM stages III–IV was significantly higher than TNM stages I–II (no data were available on HCC classification in the ICGC dataset) (P=1.1e-05, Figure 7 G). The results of multi-factor analysis were extracted from the TCGA and ICGC cohort data to establish a nomogram; the independent scores of 8 prognostic factors were verified; the corresponding probabilities were assessed on the nomogram, and the patient's 1-year probability of survival was estimated at 2 and 3 years. The nomogram performed well in predicting 1-, 2-, and 3-year survival probabilities (Figure 8 A-H).

Table 1, The risk score of the prognostic model and clinical characteristics from TCGA and ICGC database

	TCGA-LIHC			ICGC-(LIRI-JP)		
	High Risk	Low Risk	P	High Risk	Low Risk	P
Age						
≤65	112(61.54%)	115(62.84%)	0.88	44(38.26%)	45(38.79%)	1

>65	70(38.46%)	68(37.16%)		71(61.74%)	71(61.21%)	
Gender						
FEMALE	60(32.97%)	59(32.24%)	0.97	29(25.22%)	32(27.59%)	0.79
MALE	122(67.03%)	124(67.76%)		86(74.78%)	84(72.41%)	
Grade						
G1-2	98(53.85%)	132(72.13%)	2.0e-04			
G3-4	83(45.6%)	47(25.68%)				
unknow	1(0.55%)	4(2.19%)				
Stage						
I-II	112(61.54%)	142(77.6%)	9.0e-04	56(48.7%)	85(73.28%)	2.0e-04
III-IV	57(31.32%)	30(16.39%)		59(51.3%)	31(26.72%)	
unknow	13(7.14%)	11(6.01%)				

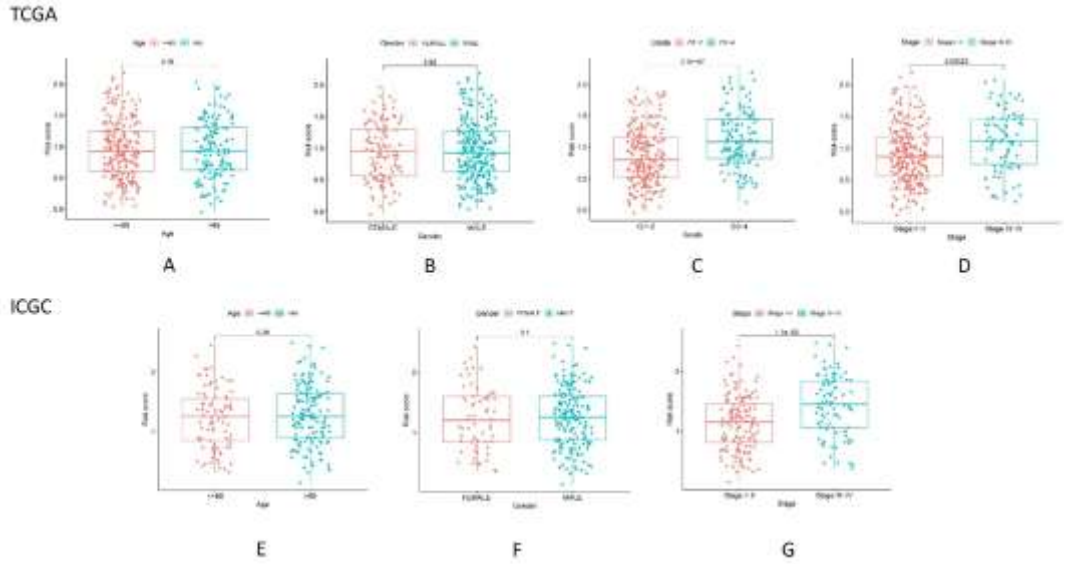

Figure 7, Risk scores for high and low risk groupings divided with clinical characteristics. (A-D): The correlation between risk score and age, gender, grade, and stage in TCGA-LIHC dataset. (E-G): The correlation between risk score and age, gender, and stage in ICGC - (LIRI-JP) dataset.

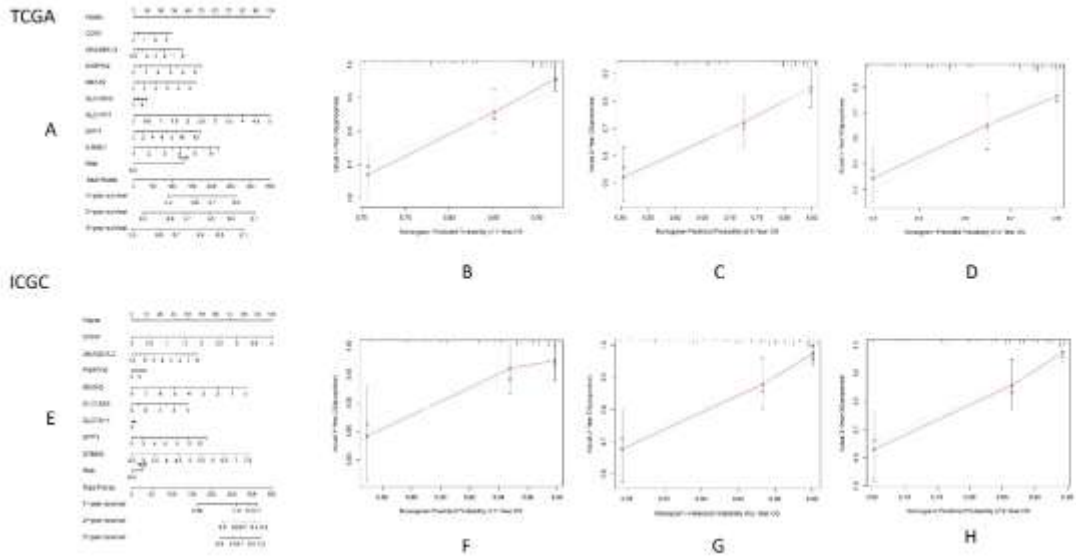

Figure 8, Nomogram based on the prognosis characteristics of the 8 genes is in HCC from TCGA

and ICGC cohort. (A, E): Build a nomogram model of 8 genes and high and low risk to predict one, two, and three years of survival. The calibration chart shows that the predicted survival rate is consistent with the actual survival rates for 1 year (B, F), 2 years (C, G), and 3 years (D, H).

3.6 Functional enrichment analyses

The GO and KEGG pathway enrichment analyses were performed on the DEGs between the high- and low-risk groups. The GO functional enrichment analysis revealed that the main pathways in which the DEGs were involved were nuclear division, chromosome segregation, and steroid hydroxylase activity. KEGG enrichment analysis revealed that the main pathways in which the DEGs were involved were Cell cycle, Human T-cell leukemia virus 1 infection, HIF-1 signaling pathway, PPAR signaling pathway, IL-17 signaling pathway, PI3K−Akt signaling pathway, and Central carbon metabolism in cancer (Figures 9 A, B). The results of the ICGC-(LIRI-JP) cohort were similar to those of the TCGA-LIHC cohort (Figures 9 C, D).

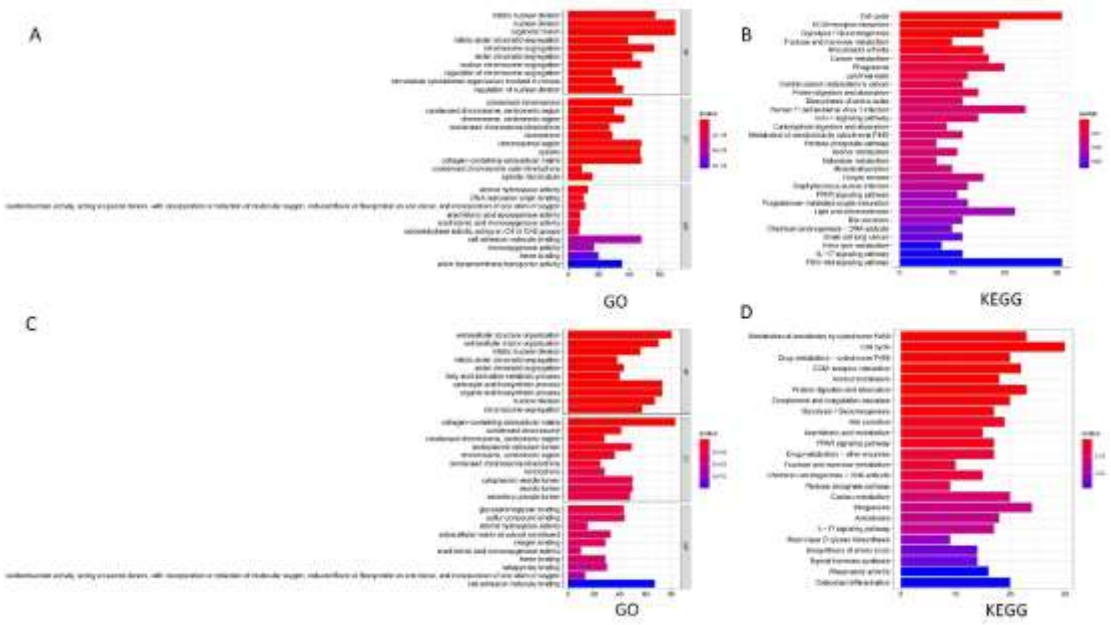

Figure 9, Functional enrichment analysis is based on DEGs between high and low risk groups in the TCGA and ICGC cohort. (A, C) GO, Gene Ontology. (B, D) KEGG, Kyoto Encyclopedia of Genes and Genomes.

3.8 Prognostic Gene Expression and Sensitivity of Cancer Cells to Chemotherapy

The expression of 8 prognosis-related genes was studied in the NCI-60 cell line, and the relationship between their expression levels and drug sensitivity was analyzed. According to the p-value, the top 16 drugs with significant sensitivity were selected for analysis and correlation with 7 genes (Figure 10). DNASE1L3, ENTPD2, MFAP2, SLC7A11, SPP1, and STMN1 were related to increased drug resistance of cancer cells to fulvestrant, ifosfamide, nelarabine, bisacodyl, active ingredient of viraplex, isotretinoin, oxaliplatin, fluphe0zine, imiquimod, megestrol acetate, hydroxyurea, dexamethasone decadron, epirubicin, and carmustine. Interestingly, the increase in SLC16A3 expression was associated with the increase in the sensitivity of cancer cells to arsenic trioxide (ATO) and ixazomib citrate.

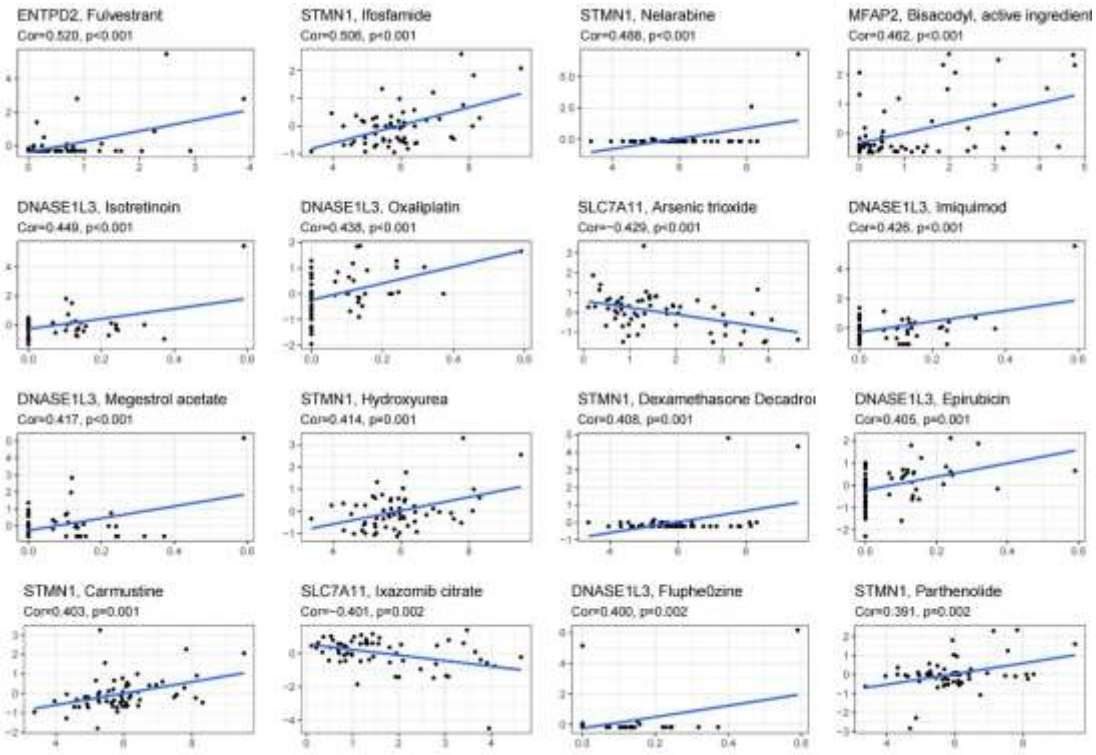

Figure 10, Scatter plot of the relationship between 8 related prognostic gene expression and drug sensitivity.

Discussion

At present, the prediction models of liver cancer related to iron death, DNA methylation, m6A methylation, long non-coding RNA, endoplasmic reticulum stress, and glycolysis have better performance [23-28]. However, the prognostic value of immune- and inflammation-related markers in serum is not studied in HCC.

In this study, a prognostic model with immune- and inflammation-related genes in TCGA-LIHC and ICGC-(LIRI-JP) was established. The prognostic model indicated that the AUC for 1, 3, and 5 years was 0.791, 0.727, and 0.718 for TCGA-LIHC and 0.730, 0.727, and 0.722 for ICGC-(LIRI-JP), respectively. Recent studies have reported that clinical features such as age, gender, tumor grade, and metastatic diagnosis are insufficient to accurately predict the outcome of patients with HCC [29]. In our study, the model divided the samples into high- and low-risk groups, both of which were significantly correlated with age, gender, tumor stage, grade. The prognostic model established in this study included 8 immune- and inflammation-related genes (*CCNF*, *DNASE1L3*, *ENTPD2*, *MFAP2*, *SLC16A3*, *SLC7A11*, *SPP1*, and *STMN1*).

DNASE1L3 is a potential biomarker for predicting the prognosis of HCC, and the positive expression of DNASE1L3 can be a key indicator of a good prognosis in liver cancer [30-31]. ENTPD2, a CD39 superfamily ectonucleotidase, orchestrates inflammatory resolution and regenerative processes through extracellular nucleotide metabolism via ATP/ADP phosphohydrolysis, modulating purinergic signaling cascades critical for tissue homeostasis [32]. MFAP2 (MAGP1) functions as a structural architect of elastic matrix assemblies, mediating fibrin-microfibril crosstalk that governs extracellular matrix biomechanical properties through calcium-dependent fibrillin interactions [33]. SLC16A3 is proven to be a downstream factor of TSTA3 immune-response-mediated metabolism coupling cell cycle and non-neoplastic hepatitis/cirrhosis tissue replication [34]. SLC7A11 is widely expressed in cells and organs such as brain, liver, macrophages, and retinal pigment cells. To inhibit cell proliferation in vitro, SLC7A11 overexpression may be related to the advanced pathological stage of HCC [35]. Secreted phosphoprotein 1 (SPP1) are associated with many malignant characteristics in cancer, such as epithelial-mesenchymal plasticity, cancer stem cell (CSC) resistance, and chemotherapy and

radiotherapy resistance in HCC [36]. STMN1 is an oncogene encoding a highly conserved cytoplasmic phosphorylated 18-kDa protein, and it can promote cell differentiation, proliferation, and migration. It is upregulated in numerous cancers, including non-small cell lung cancer, breast cancer, liver cancer, and gastric cancer [37]. Therefore, we suggested that these genes can be used as novel biomarkers for the treatment of HCC.

CSCs can impact the recurrence, metastasis, and resistance in HCC [38]. HIF-1, Akt, and IL-17 signaling pathways can increase the proportion of CSCs, leading to immunosuppression in HCC [39]. In this study, MFAP2 was negatively correlated with RNAss and DNAss, and STMN1 was positively correlated with RNAss and DNAss. This indicated that MAPF2 may inhibit and STMN1 may promote the differentiation of CSCs. DNASE1L3, MFAP2, SLC16A3, and SPP1 were positively correlated with the immune score, indicating that they may be related to interstitial and immune cells [40-42].

Pharmacogenomic profiling of NCI-60 cell lines revealed chemoresistance patterns correlating with transcriptional upregulation of specific prognostic biomarkers. Enhanced DNASE1L3 expression conferred therapeutic refractoriness to oxaliplatin-based regimens (sorafenib/5-FU/leucovorin) in HCC patients with portal vein invasion, as evidenced in phase III clinical trials [43]. Conversely, SLC711 overexpression potentiated arsenic trioxide (ATO) sensitivity through cancer stem cell (CSC) differentiation via epigenetic reprogramming of pluripotency networks. Synergistic efficacy was observed in ATO-5FU/cisplatin combinatorial therapy, mechanistically involving dual blockade of oncogenic LIF-JAK/STAT3 and NF-κB signaling axes that sustain CSC self-renewal capacities [44].

Conclusion

In this study, 8 immune- and inflammation-related genes in TCGA-LIHC and ICGC-(LIRI-JP) were screened, and a novel prognostic model was established. These genes may play a role in the development and progression of HCC, and the underlying mechanisms related to immunity and inflammation should be further studied. Simultaneous, we construction of predictive models and TME and drug resistance may provide effective and safe strategies for chemotherapy and immunotherapy in HCC.

Acknowledgments: No applicable

Authors Contributions

XF and WL conceived and designed the project. YX and YT acquired, analyzed, and interpreted the data. All authors wrote and revised the paper.

Funding

This work was supported by Health Research Project of Hunan Provincial Health Commission (grant number: D202304017818)

Data available

All data in this study can be obtained by contacting the corresponding author.

The raw data of this study are derived from the TCGA database (https://portal.gdc.cancer.gov/) and International Cancer Genome Consortium (ICGC) Database (https://dcc.icgc.org/), which are publicly available databases.

Ethics approval and consent to participate: Not applicable.

Consent for publication: Not applicable.

Competing Interests: All authors declare no competing interest.

Reference

1. Siegel RL, Miller KD, Wagle NS, Jemal A. Cancer statistics, 2023. *CA Cancer J Clin*. 2023;73(1):17-48.
2. Yang JD, Hainaut P, Gores GJ, Amadou A, Plymoth A, Roberts LR. A global view of hepatocellular carcinoma: trends, risk, prevention and management. *Nat Rev Gastroenterol Hepatol*. 2019;16(10):589-604.
3. Alqahtani A, Khan Z, Alloghbi A, Said Ahmed TS, Ashraf M, Hammouda DM. Hepatocellular Carcinoma: Molecular Mechanisms and Targeted Therapies . *Medicina (Kaunas)*. 2019;55(9):526.
4. Yang JD, Hainaut P, Gores GJ, Amadou A, Plymoth A, Roberts LR. A global view of hepatocellular carcinoma: trends, risk, prevention and management. *Nat Rev Gastroenterol Hepatol*. 2019;16(10):589-604.
5. Zhang H, Ye Y, Li W. Perspectives of Molecular Therapy-Targeted Mitochondrial

Fission in Hepatocellular Carcinoma. *Biomed Res Int*. 2020;2020:1039312.
6. Choi C, Yoo GS, Cho WK, Park HC. Optimizing radiotherapy with immune checkpoint blockade in hepatocellular carcinoma. *World J Gastroenterol*. 2019;25 (20): 2416-2429.
7. Satilmis B, Sahin TT, Cicek E, Akbulut S, Yilmaz S. Hepatocellular Carcinoma Tumor Microenvironment and Its Implications in Terms of Anti-tumor Immunity: Future Perspectives for New Therapeutics. *J Gastrointest Cancer*. 2021;52(4):1198-1205.
8. Vogel A, Meyer T, Sapisochin G, Salem R, Saborowski A. Hepatocellular carcinoma . *Lancet*. 2022;400(10360):1345-1362.
9. Hibino S, Kawazoe T, Kasahara H, et al. Inflammation-Induced Tumorigenesis and Metastasis. *Int J Mol Sci*. 2021;22(11):5421. Published 2021 May 21.
10. Greten FR, Grivennikov SI. Inflammation and Cancer: Triggers, Mechanisms, and Consequences. *Immunity*. 2019;51(1):27-41.
11. Zaidi MR. The Interferon-Gamma Paradox in Cancer. *J Interferon Cytokine Res*. 2019;39(1) :30-38.
12. Sistigu A, Di Modugno F, Manic G, Nisticò P. Deciphering the loop of epithelial-mesenchymal transition, inflammatory cytokines and cancer immunoediting. *Cytokine Growth Factor Rev*. 2017;36:67-77.
13. Xiao N, Zhu X, Li K, Chen Y, Liu X, Xu B, et al. Blocking siglec-10^{hi} tumor-associated macrophages improves anti-tumor immunity and enhances immunotherapy for hepatocellular carcinoma. Exp Hematol Oncol . 2021 Jun 10;10(1):36.
14. Liu Y, Cao X. Immunosuppressive cells in tumor immune escape and metastasis. *J Mol Med (Berl)*. 2016;94(5):509-522.
15. Mandal A, Viswanathan C. Natural killer cells: In health and disease. *Hematol Oncol Stem Cell Ther*. 2015;8(2):47-55.
16. Abel AM, Yang C, Thakar MS, Malarkannan S. Natural Killer Cells: Development, Maturation, and Clinical Utilization. *Front Immunol*. 2018;9:1869.
17. Morvan MG, Lanier LL. NK cells and cancer: you can teach innate cells new tricks. *Nat Rev Cancer*. 2016;16(1):7-19. doi:10.1038/nrc.2015.5
18. Han C, Jiang Y, Wang Z, Wang H. Natural killer cells involved in tumour immune escape of hepatocellular carcinomar. *Int Immunopharmacol*. 2019;73:10-16.
19. Liu C, Wang X, Genchev GZ, Lu H. Multi-omics facilitated variable selection in Cox-regression model for cancer prognosis prediction. *Methods*. 2017;124:100-107.
20. Li C, Pak D, Todem D. Adaptive lasso for the Cox regression with interval censored and possibly left truncated data. *Stat Methods Med Res*. 2020;29(4):1243-1255.
21. Subramanian A, Tamayo P, Mootha VK, Mukherjee S, Ebert BL, Gillette MA, et al. Gene set enrichment analysis: a knowledge-based approach for interpreting genome-wide expression profiles. Proc Natl Acad Sci U S A. 2005 Oct 25;102(43):15545-50.
22. Yoshihara K, Shahmoradgoli M, Martínez E, Vegesna R, Kim H, Torres-Garcia W, et al. Inferring tumour purity and stromal and immune cell admixture from expression data. Nat Commun. 2013;4:2612.
23. Deng T, Hu B, Jin C, Tong Y, Zhao J, Shi Z, et al. A novel ferroptosis phenotype-related clinical-molecular prognostic signature for hepatocellular carcinoma. J Cell Mol Med. 2021 Jul;25(14):6618-6633.
24. Bai Y, Tong W, Xie F, Zhu L, Wu H, Shi R, et al. DNA methylation biomarkers for diagnosis of primary liver cancer and distinguishing hepatocellular carcinoma from intrahepatic cholangiocarcinoma. Aging (Albany NY). 2021 Jul 8;13(13):17592-17606.
25. Du Y, Ma Y, Zhu Q, Liu T, Jiao Y, Yuan P, et al. An m6A-Related Prognostic Biomarker Associated With the Hepatocellular Carcinoma Immune Microenvironment. Front Pharmacol. 2021 Jun 24;12:707930.
26. Ma W, Yao Y, Xu G, Wu X, Li J, Wang G, Chen X, et al. Identification of a seven-long non-coding RNA signature associated with Jab1/CSN5 in predicting hepatocellular carcinoma. Cell Death Discov. 2021 Jul 10; 7(1):178.
27. Liu P, Wei J, Mao F, Xin Z, Duan H, Du Y, et al. Establishment of a Prognostic Model for Hepatocellular Carcinoma Based on Endoplasmic Reticulum Stress-Related Gene Analysis. Front Oncol. 2021 May 21;11:641487.
28. Jiang L, Zhao L, Bi J, Guan Q, Qi A, Wei Q,

et al. Glycolysis gene expression profilings screen for prognostic risk signature of hepatocellular carcinoma. Aging (Albany NY). 2019 Dec 2;11(23):10861-10882.
29. Yu TH, Chen X, Zhang XH, Zhang EC, Sun CX. Clinicopathological characteristics and prognostic factors for intrahepatic cholangiocarcinoma: a population-based study. *Sci Rep*. 2021;11(1):3990.
30. Guo D, Ma D, Liu P, Lan J, Liu Z, Liu Q. DNASE1L3 arrests tumor angiogenesis by impairing the senescence-associated secretory phenotype in response to stress. *Aging (Albany NY)*. 2021;13(7):9874-9899.
31. Wang S, Ma H, Li X, Mo X, Zhang H, Yang L, et al. DNASE1L3 as an indicator of favorable survival in hepatocellular carcinoma patients following resection. Aging (Albany NY). 2020 Jan 24;12(2):1171-1185.
32. Feldbrügge L, Jiang ZG, Csizmadia E, Mitsuhashi S, Tran S, Yee EU, et al. Distinct roles of ecto-nucleoside triphosphate diphosphohydrolase-2 (NTPDase2) in liver regeneration and fibrosis. Purinergic Signal. 2018 Mar;14(1):37-46.
33. Craft CS, Broekelmann TJ, Mecham RP. Microfibril-associated glycoproteins MAGP-1 and MAGP-2 in disease. *Matrix Biol*. 2018; 71-72:100-111.
34. Wang L, Huang J, Jiang M, Lin H. Tissue-specific transplantation antigen P35B (TSTA3) immune response-mediated metabolism coupling cell cycle to postreplication repair network in no-tumor hepatitis/cirrhotic tissues (HBV or HCV infection) by biocomputation. *Immunol Res*. 2012;52(3):258-268.
35. Zhang L, Huang Y, Ling J, Zhuo W, Yu Z, Luo Y, et al. Overexpression of SLC7A11: a novel oncogene and an indicator of unfavorable prognosis for liver carcinoma. Future Oncol. 2018 Apr;14(10):927-936.
36. Gao S, Gang J, Yu M, Xin G, Tan H. Computational analysis for identification of early diagnostic biomarkers and prognostic biomarkers of liver cancer based on GEO and TCGA databases and studies on pathways and biological functions affecting the survival time of liver cancer. *BMC Cancer*. 2021;21 (1):791.
37. Zhang ED, Li C, Fang Y, Li N, Xiao Z, Chen C, et al. STMN1 as a novel prognostic biomarker in HCC correlating with immune infiltrates and methylation. World J Surg Oncol. 2022 Sep 20;20(1):301.
38. Yang XD, Kong FE, Qi L, Lin JX, Yan Q, Loong JHC, et al. PARP inhibitor Olaparib overcomes Sorafenib resistance through reshaping the pluripotent transcriptome in hepatocellular carcinoma. Mol Cancer. 2021 Jan 23;20(1):20.
39. Dai X, Guo Y, Hu Y, Bao X, Zhu X, Fu Q, et al. Immunotherapy for targeting cancer stem cells in hepatocellular carcinoma. Theranostics. 2021 Jan 19;11(7):3489-3501.
40. Liu J, Yi J, Zhang Z, Cao D, Li L, Yao Y. Deoxyribonuclease 1-like 3 may be a potential prognostic biomarker associated with immune infiltration in colon cancer. *Aging (Albany NY)*. 2021;13(12):16513-16526.
41. Wang L, Huang J, Jiang M, Lin H. Tissue-specific transplantation antigen P35B (TSTA3) immune response-mediated metabolism coupling cell cycle to postreplication repair network in no-tumor hepatitis/cirrhotic tissues (HBV or HCV infection) by biocomputation. *Immunol Res*. 2012;52(3):258-268.
42. Dai X, Guo Y, Hu Y, Bao X, Zhu X, Fu Q, et al. Immunotherapy for targeting cancer stem cells in hepatocellular carcinoma. Therano stics. 2021 Jan 19;11(7):3489-3501. doi: 10.7150/thno.54648. PMID: 33537099; PMCID: PMC7847682.
43. He M, Li Q, Zou R, Shen J, Fang W, Tan G, Zhou Y, Wu X, Xu L, Wei W, Le Y, Zhou Z, Zhao M, Guo Y, Guo R, Chen M, Shi M. Sorafenib Plus Hepatic Arterial Infusion of Oxaliplatin, Fluorouracil, and Leucovorin vs Sorafenib Alone for Hepatocellular Carcinoma With Portal Vein Invasion: A Randomized Clinical Trial. JAMA Oncol. 2019 Jul 1;5(7):953-960.